[AMERICAN JOURNAL OF SCIENCE, SCHAIRER VOL. 267-A, 1969, P. 463-479]

PHASE EQUILIBRIA IN THE SYSTEM MgO–IRON OXIDE–TiO_2 IN AIR*

E. WOERMANN, B. BREŽNY and A. MUAN**

ABSTRACT. Phase relations in the system MgO–iron oxide–TiO_2 in air have been determined by the quenching technique. The phase diagram for the bounding binary system MgO–TiO_2 has been revised with respect to the melting relations of the various compounds appearing in this system. The compounds Mg_2TiO_4 (spinel) and $MgTiO_3$ (rhombohedral phase = geikielite) melt incongruently at 1756 and 1630°C, respectively, whereas $MgTi_2O_5$ (Mg-pseudobrookite) melts congruently at 1662°C. The liquidus surface of the system MgO–iron oxide–TiO_2 shows large primary-phase areas of spinel and pseudobrookite solid solutions extending continuously across the diagram from the MgO–TiO_2 side to the iron oxide–TiO_2 side. In contrast to this, the primary phase areas of the rhombohedral phases (geikielite solid solution and hematite solid solution) are restricted to areas adjacent to the two bounding systems MgO–TiO_2 and iron oxide–TiO_2 at liquidus temperatures in air. In the central part of the system, the rhombohedral phases are unstable relative to the phase assemblage spinel plus pseudobrookite.

INTRODUCTION

Relatively few equilibrium data are available for TiO_2–containing systems. The present work represents an attempt to expand our knowledge of the behavior of TiO_2 in oxide phases by studying combinations of this component with other components of importance in geological sciences and technology, namely, MgO and iron oxide.

The present study was carried out in air. Under these conditions, the iron is present partly in the divalent state and partly in the trivalent state in varying amounts, and therefore, the system is not ternary. However, the choice of a constant oxygen pressure of the gas phase (P_{O_2} = 0.2 atm) expends 1 degree of freedom, and hence the system may be treated like a ternary system. The phase relations are then conveniently represented in a triangular diagram, as described in detail previously (Muan and Osborn, 1956, 1965).

The oxygen pressure and temperatures selected in this study are much higher than those prevailing in natural rock-forming systems. However, it is felt that fundamental data obtained under experimentally favorable conditions will serve as a reliable starting point for ascertaining trends in the role of titania in important types of mineral structures. It is significant that the oxygen pressure selected in this study is high enough that essentially all titanium will be present in the tetravalent state as can be derived from stability data available for the various oxides of titanium (Elliott and Gleiser, 1960).

Phase equilibrium data are available for the "binary" systems bounding the present "ternary" system. The phase diagram for the system MgO–iron oxide in air is shown in figure 1, after Phillips, Sōmiya, and

* Contribution No. 67-54 from College of Earth and Mineral Sciences, The Pennsylvania State University, University Park, Pa. 16802

** At the time this work was done, the authors were Research Fellow, Research Associate and Professor of Mineral Sciences, respectively, in the College of Earth and Mineral Sciences at The Pennsylvania State University. E. Woermann is now with the University of Frankfurt, Germany, and B. Brezny is with the Refractories Research Institute, Bratislava, Czechoslovakia.

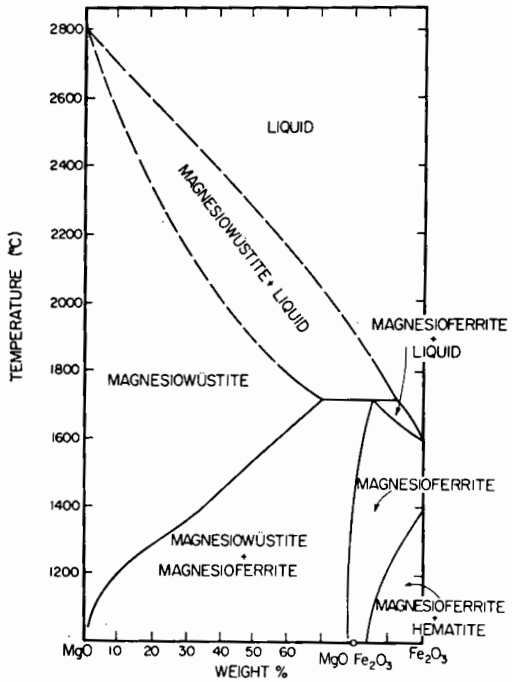

Fig. 1. Phase diagram for the system MgO–iron oxide in air (Phillips, Sōmiya, and Muan, 1961). The system is not binary because iron occurs in two different oxidation states (Fe^{2+} and Fe^{3+}) in varying amounts. Compositions of condensed phases have been projected along oxygen reaction lines (Muan and Osborn, 1956, 1965) onto the join $MgO–Fe_2O_3$.

Muan (1961). The essential features of this diagram have been confirmed recently by Willshee and White (1967). The phase diagram for the system iron oxide–TiO_2 in air shown in figure 2, after MacChesney and Muan (1959).

There is still considerable uncertainty in the literature regarding some of the features of phase relations in the system $MgO–TiO_2$, as shown in the two different versions of the diagram for this system reproduced in figure 3. The diagram on the left (fig. 3A) is after Coughanour and DeProsse (1953) and the diagram on the right (fig. 3B) after Massazza and Sirchia (1958). It is seen that whereas the former authors portray all three compounds in the system (Mg_2TiO_4, $MgTiO_3$, and $MgTi_2O_5$) as melting congruently, the latter authors show Mg_2TiO_4 and $MgTiO_3$ as melting incongruently.

EXPERIMENTAL METHODS

The quenching method used in this investigation has been described repeatedly in the literature since its introduction some 60 years ago (Shepherd, Rankin, and Wright, 1909), and only specific details pertinent to the present investigation will be described here.

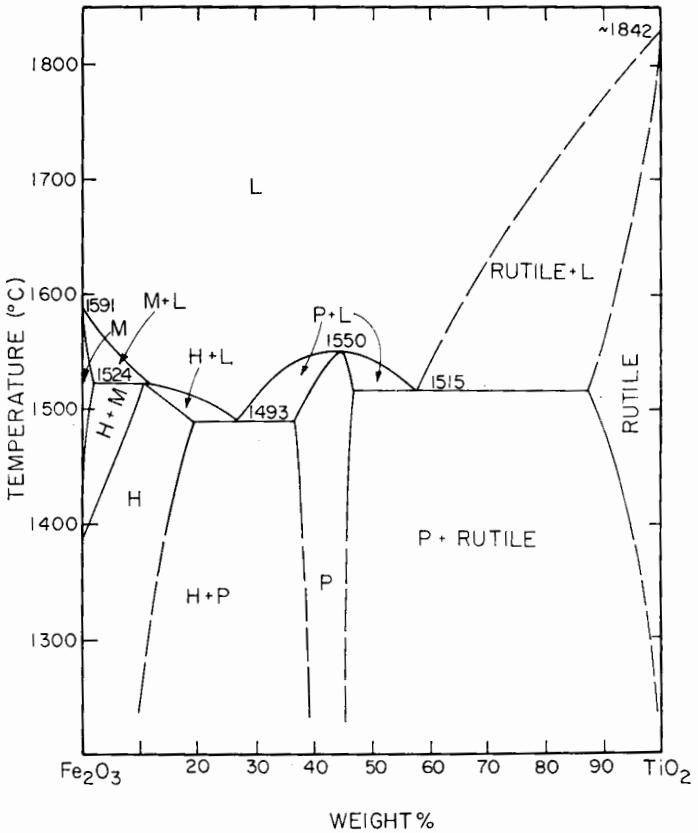

Fig. 2. Phase diagram for the system iron oxide–TiO_2 in air (MacChesney and Muan, 1959). The system is not binary because iron occurs in two different oxidation states (Fe^{2+} and Fe^{3+}) in varying amounts. Compositions of condensed phases have been projected along oxygen reaction lines (Muan and Osborn, 1956, 1965) onto the join Fe_2O_3–TiO_2. Abbreviations used have the following meanings: M = magnetite solid solution, H = hematite solid solution, P = pseudobrookite solid solution, L = liquid.

The starting materials were reagent-grade chemicals ("Fisher Certified" reagents). The oxide mixtures were pre-heated for ~24 hrs in a globar furnace at ~1400°C prior to final equilibration. This pre-heating promoted partial or complete reaction of the oxide components to form an aggregate of the appropriate crystalline titanate phases prior to the final equilibration runs.

Attainment of equilibrium in the latter runs was checked by approaching the equilibrium from above and from below in selected samples and by varying the time of equilibration. It was found that 4 to 6 hours were sufficient for runs in which a liquid phase was present, whereas considerably longer times were required in most of the equilibration runs at subsolidus temperatures, particularly at the lower tem-

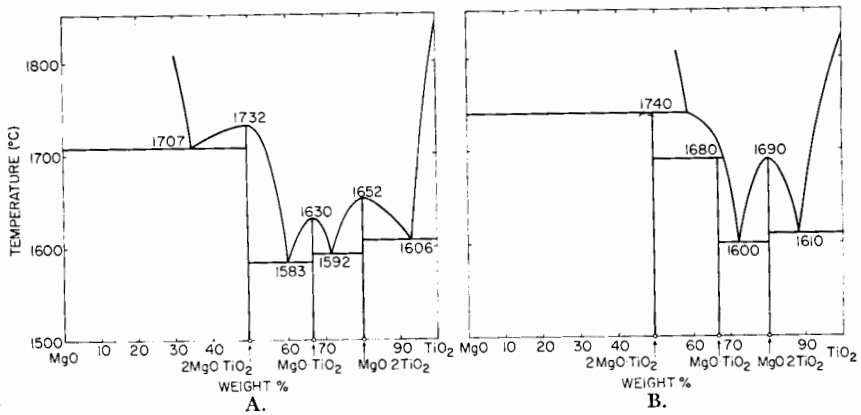

Fig. 3. Phase diagrams for the system $MgO–TiO_2$ as reported in previous literature. The diagram on the left is after Coughanour and DeProsse (1953), and the diagram on the right is after Massazza and Sirchia (1958).

peratures (1300 and 1000°C). The equilibration times are given for each sample in subsequent tables summarizing results of equilibration runs at subsolidus temperatures. Equilibration runs up to ~1550°C were carried out in vertical tube furnaces with 80 percent Pt 20 percent Rh windings, and equilibration runs at higher temperatures were carried out in vertical tube furnaces with Mo windings. Constancy of temperatures to approximately ± 3°C during the runs was maintained by commercial electronic controllers. Temperatures up to 1550°C were measured with Pt versus 90 percent Pt 10 percent Rh thermocouples, and higher temperatures were measured with 95 percent Pt 5 percent Rh versus 80 percent Pt 20 percent Rh thermocouples. The theromocouples were calibrated against the following fixed points: diopside, 1391.5°C; pseudowollastonite, 1546°C; liquidus temperature of a 90 percent SiO_2 10 percent CaO mixture, 1707°C. Temperatures so defined are in accordance with the 1948 International Scale (Sosman, 1952). The temperatures reported in subsequent tables and text are estimated to be accurate to ± 5°C or better up to 1550°C, and to ± 10°C or better at higher temperatures.

RESULTS

The system $MgO–TiO_2$.—Results of equilibration runs in the system $MgO–TiO_2$ are shown in table 1 and illustrated graphically in figure 4. The data establish the presence of two peritectic points and two eutectic points in this system, thus confirming the general relations determined by Massazza and Sirchia (1958) (figure 3B). However, the temperatures observed in the two investigations differ considerably. The liquidus invariant points, as determined in the present investigation, are listed on the next page.

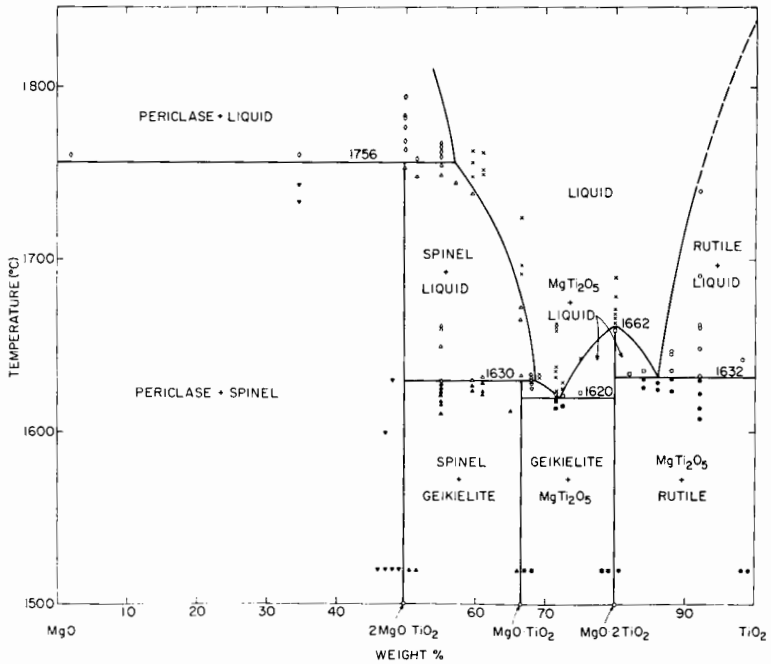

Fig. 4. Phase diagram for the system MgO–TiO_2 as determined in the present investigation.

Temperature, °C	Phases present
1756	Periclase, Mg_2TiO_4, liquid (43 wt percent MgO, 57 wt percent TiO_2)
1630	Mg_2TiO_4, $MgTiO_3$, liquid (32 wt percent MgO, 68 wt percent TiO_2)
1620	$MgTiO_3$ $MgTi_2O_5$, liquid (28 wt percent MgO, 72 wt percent TiO_2)
1632	$MgTi_2O_5$, TiO_2, liquid (14 wt percent MgO, 86 wt percent TiO_2)

The system MgO–Iron Oxide–TiO_2 in air.—Results of equilibration runs in the liquidus-solidus temperature region of the system MgO–iron oxide–TiO_2 in air are listed in table 2 and shown graphically in figures 5 and 6. The first of these diagrams (fig. 5) is a projection of the liquidus surface, showing compositions of mixtures studied, boundary curves separating the various primary-phase areas, and liquidus isotherms. The second diagram (fig. 6) is a projection of the solidus surface, showing the crystalline phases coexisting with a trace of liquid at solidus temperatures in the various composition areas of the system, and the solidus temperatures. The solidus isotherms are straight lines in areas where

TABLE 1

Results of equilibration runs in the system MgO-TiO_2

Composition, wt percent MgO	Composition, wt percent TiO_2	Temp., °C	Phases present
98.0	2.0	1760	MgO + tr L
65.5	34.5	1760	MgO + L
		1743	MgO + S
		1733	MgO + S
54.0	46.0	1520	MgO + S
53.0	47.0	1600	MgO + S
		1520	MgO + S
52.0	48.0	1630	MgO + S
		1520	MgO + S
51.0	49.0	1520	MgO + S
50.2	49.8	1795	MgO + L
		1783	MgO + L
		1782	MgO + L
		1777	MgO + L
		1769	MgO + L
		1764	MgO + L
		1753	S + minor MgO
			G + minor L
49.5	50.5	1520	S + G
48.5	51.5	1520	S + G
48.0	52.0	1758	MgO + L
		1748	S + L
44.5	55.5	1782	L
		1767	MgO + L
		1765	MgO + L
		1762	MgO + L
		1758	MgO + S + L
		1755	S + L
		1755	S + L
		1749	S + L
		1749	S + L
		1663	S + L
		1660	S + L
		1660	S + L
		1650	S + L
		1630	S + L
		1628	S + G
		1626	S + G
		1625	S + G
		1624	S + G
		1622	S + G
		1618	S + G
		1616	S + G
		1611	S + G
43.0	57.0	1755	S + L
41.0	59.0	1763	L
		1756	S
		1748	S
		1739	S + L
		1631	S + L
		1627	G + S
		1624	G + S
39.0	61.0	1762	L
		1752	L
		1749	L
		1633	S + L
39.0	61.0	1629	S
		1623	G + S
		1622	G + S
35.0	65.0	1612	G + S
34.0	66.0	1520	S + G
33.5	66.5	1724	L
		1698	L
		1692	L
		1673	S + L
		1666	minor S + L
		1633	tr S + L
	67.0	1520	G + $MgTi_2O_5$
32.0	68.0	1634	S + L
		1633	S + L
		1632	S + L
		1629	G + L
		1628	G + L
		1625	G + L
		1520	G + $MgTi_2O_5$
31.0	69.0	1634	L
		1632	L
28.5	71.5	1663	L
		1661	L
		1660	L
		1638	L
		1637	L
		1632	L
		1626	L
		1623	L
		1622	G + L
		1618	G + $MgTi_2O_5$
		1614	G + $MgTi_2O_5$
		1614	G + $MgTi_2O_5$
27.5	72.5	1629	L
		1625	L
		1621	$MgTi_2O_5$
		1615	G + $MgTi_2O_5$
25.0	75.0	1643	L
		1623	$MgTi_2O_5$ + L
22.0	78.0	1520	G + $MgTi_2O_5$
21.0	79.0	1520	G + $MgTi_2O_5$
20.2	79.8	1691	L
		1679	L
		1672	L
		1669	L
		1667	L
		1664	L
		1660	$MgTi_2O_5$
19.5	80.5	1520	$MgTi_2O_5$ + R
18.0	82.0	1634	$MgTi_2O_5$ + L
		1618	$MgTi_2O_5$ + R
16.0	84.0	1636	$MgTi_2O_5$ + L
		1631	$MgTi_2O_5$ + R
		1626	$MgTi_2O_5$ + R

TABLE 1 (continued)

Composition, wt percent		Temp., °C	Phases present	Composition, wt percent		Temp., °C	Phases present
MgO	TiO_2			MgO	TiO_2		
14.0	86.0	1629	$MgTi_2O_5$ + R	8.0	92.0	1661	R + L
		1625	$MgTi_2O_5$ + R			1649	R + L
						1633	R + L
12.0	88.0	1647	R + L			1631	R + $MgTi_2O_5$ + tr L
		1645	R + L			1623	$MgTi_2O_5$ + R
		1636	R + L			1614	$MgTi_2O_5$ + R
		1629	$MgTi_2O_5$ + R + tr L			1608	$MgTi_2O_5$ + R
		1624	$MgTi_2O_5$ + R				
				2.0	98.0	1643	R + L
8.0	92.0	1740	minor R + L			1520	$MgTi_2O_5$ + R
		1691	R + L				
		1663	R + L	1.0	99.0	1520	$MgTi_2O_5$ + R

Abbreviations: R, rutile; G, $MgTiO_3$; S, Mg_2TiO_4; L, liquid; tr, trace.

two crystalline phases coexist with liquid, and the solidus temperature is constant in each composition triangle within which three crystalline phases coexist with liquid.

There are two liquidus "invariant"[1] points in the system MgO–iron oxide–TiO_2 in air, with temperatures and phase assemblages as follows:

Temperature, °C	Phases present
1596	α (geikielite solid solution), pseudobrookite solid solution, spinel solid solution, liquid (26 wt percent MgO, 65 wt percent TiO_2, 9 wt percent Fe_3O_2)[2]
1530	α' (hematite solid solution), pseudobrookite solid solution, spinel solid solution, liquid (7 wt percent MgO, 28 wt percent TiO_2, 65 wt percent, Fe_2O_3)[2]

Data obtained at subsolidus temperatures in the system MgO–iron oxide–TiO_2 in air are listed in table 3 and shown graphically in figures 7 to 9. Figures 7 and 8 show isothermal sections through the system at 1300°C and 1000°C, respectively, and figure 9 shows the extent of the magnesiowüstite solid solution as a function of temperature.

Among the noteworthy features of the phase relations in the system MgO–iron oxide–TiO_2 in air at a total pressure of 1 atm is the instability of the rhombohedral phase relative to the phase assemblage spinel plus pseudobrookite in the central part of the system in the temperature range of the present investigation. However, it is seen that with decreasing temperature the extent of the rhombohedral solid solutions

[1] These points are characterized by the coexistence of three crystalline phases, liquid, and gas (P_{O_2}=0.2 atm). Because 1 degree of freedom has been expended by our choosing the constant oxygen pressure of the gas phase, the situation is similar to that prevailing at an invariant point.

[2] Total iron oxide calculated as Fe_2O_3.

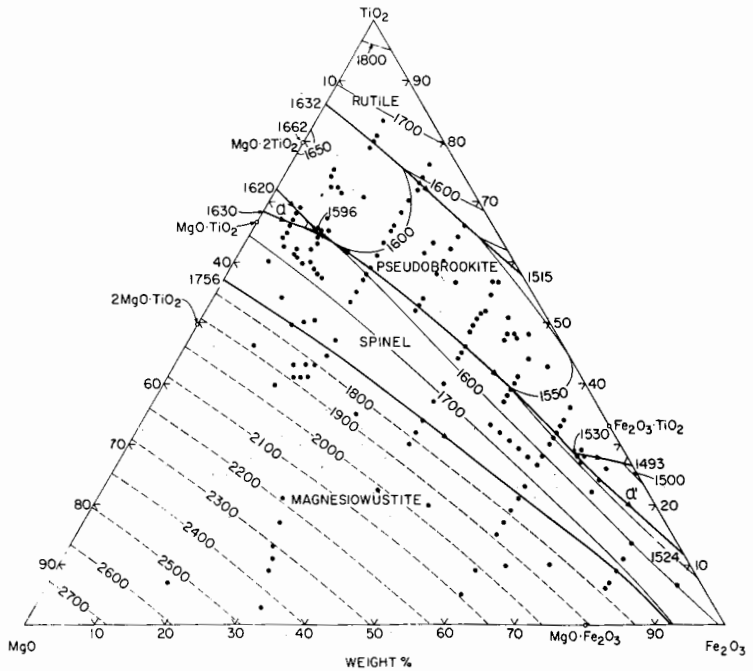

Fig. 5. Projection of the liquidus surface of the system MgO–iron oxide–TiO_2 in air. Abbreviations used have the following meanings: α = geikielite solid solution, α' = hematite solid solution.

increases (note the relatively small area of coexistence of spinel and pseudobrookite in the 1000°C isothermal section of fig. 8). A reasonable extrapolation of the data to lower temperatures indicates that the phase assemblage spinel + pseudobrookite in air probably is unstable below ~700°C. Similarly it may be inferred that two rhombohedral phases (α and α') probably will coexist in equilibrium in the system MgO–iron oxide–TiO_2 in air at low temperatures (below ~700°C). Quantitative determination of stability interrelations of these phases at temperatures below those used in the present investigation appears to be an interesting problem for future experimental study. Inasmuch as the reactions in the dry system are quite sluggish at 1000°C (note that equilibration times at this temperature were up to 500 hr), it is not considered practical to extend the present work to much lower temperatures with the techniques used in this investigation. It is suggested that these relations at lower temperatures might be studied by hydrothermal techniques.

Another noteworthy feature of phase relations in the system MgO–iron oxide–TiO_2 in air is the large extent of the stability field of mag-

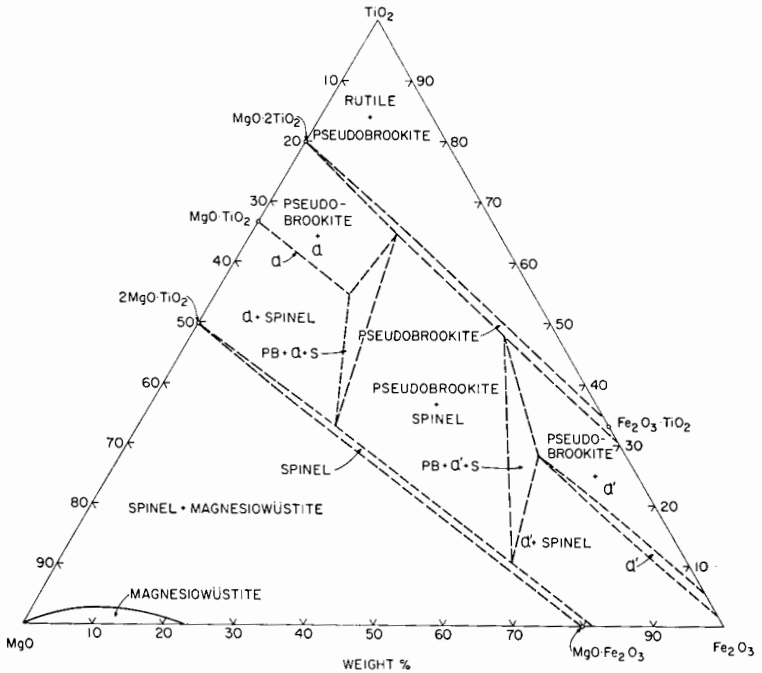

Fig. 6. Projection of the solidus surface of the system MgO–iron oxide–TiO_2 in air. Abbreviations used have the following meanings: α = geikielite solid solution, α' = hematite solid solution, PB = pseudobrookite solid solution.

nesiowüstite solid solutions at high temperatures and the large effect of temperature on the extent of this field. Phase-equilibrium studies (Woermann and Muan, unpub. data) of the system at much lower oxygen pressures ($P_{O_2}=10^{-8}$ atm) have shown that there is no comparable stability field for the magnesiowüstite solid solutions under strongly reducing conditions. The solubility of TiO_2 in magnesiowüstite is thus not only a function of temperature (as shown in fig. 9) but also of oxygen pressure of the atmosphere. These relations are of considerable practical interest in the technology of basic brick, in which magnesiowüstite and spinel phases commonly coexist and change in relative amounts in response to changes in temperature or oxygen pressure of the atmosphere, or both. The present data provide an important guide to the reactions that may take place in magnesite bodies in the presence of iron oxide and relatively small amounts of TiO_2. In addition, the extensive field of magnesiowüstite solid solutions is of considerable interest from a crystal-chemical standpoint, particularly with respect to the nature of the defects present. However, a detailed study of the properties of this phase is beyond the scope of the present work.

TABLE 2

Results of equilibration runs in the liquidus-solidus temperature range of the system MgO-iron oxide-TiO_2 in air

Composition, wt percent			Temp., °C	Phases present
MgO	TiO_2	Fe_2O_3*		
3.4	6.6	90.0	1529	S + L
			1523	α' + S
4.0	26.0	70.0	1527	α' + L
			1523	α' + L
			1518	α' + P + tr L
4.0	36.0	60.0	1534	L
			1527	P + L
			1506	α' + P
4.0	42.7	53.3	1565	L
			1559	P + tr L
			1552	P + α'
			1535	P + α'
4.0	48.0	48.0	1520	P
4.0	56.5	39.5	1535	P + tr L
			1529	P + tr R
4.0	66.0	30.0	1570	L
			1563	tr P + L
			1558	P + R
4.0	76.0	20.0	1570	R + P
4.8	56.8	38.4	1535	P + R
5.5	50.7	43.8	1511	P
6.0	24.0	70.0	1528	S + L
			1525	α' + minor L
6.0	29.0	65.0	1529	L
			1522	α' + P
			1513	α' + P
6.0	34.0	60.0	1534	L
			1532	P + L
			1527	α' + P + L
			1520	α' + P
6.0	44.0	50.0	1527	P + tr α' + L
			1520	P + α'
6.0	47.3	46.7	1582	L
6.0	49.0	45.0	1511	P + tr
6.0	54.5	39.5	1535	P
6.0	64.0	30.0	1569	P + L
6.0	74.0	20.0	1630	L
			1598	tr R + L
6.7	13.3	80.0	1566	S + L
			1523	α' + S
7.0	28.0	65.0	1529	L
			1522	α' + P
			1513	α' + P
7.0	33.0	60.0	1535	tr P + L
7.0	48.0	45.0	1511	P + α'
7.0	73.0	20.0	1596	L
			1594	R + P + L
7.0	83.2	9.8	1610	R + L
			1570	P + R
7.9	71.8	20.3	1596	P + L
8.0	22.0	70.0	1528	minor S + L
			1517	α' + S
8.0	32.0	60.0	1533	L
			1532	tr P + L + tr S
			1530	α' + P + tr L
			1503	P + α'
8.0	47.0	45.0	1511	P + α'
8.0	62.0	30.0	1553	P + tr R
			1537	P + minor R
8.1	51.9	40.0	1582	L
9.0	11.0	80.0	1539	S + L
9.0	31.0	60.0	1533	L
			1526	P + α'
9.0	41.0	50.0	1520	α' + P
9.0	81.2	9.8	1608	R + L
9.1	51.4	39.5	1570	L
			1535	P + α' + tr L
			1530	P + α'
10.0	30.0	60.0	1551	S + L
			1541	S + L
			1538	S + L
			1531	α' + S
10.0	40.0	50.0	1555	L
			1551	P + L
			1522	P + α'
10.0	50.5	39.5	1514	P + S
10.0	60.0	30.0	1553	P
			1537	P
10.0	63.0	27.0	1553	P
			1535	P
10.0	70.0	20.0	1599	P + tr L
			1588	P + R
10.0	80.0	10.0	1608	P + R + minor L
10.1	56.6	33.3	1603	P + L
11.0	9.0	80.0	1719	L
11.0	39.0	50.0	1554	tr S + L
			1520	P + α'
11.0	79.2	9.8	1606	P + L

TABLE 2 (continued)

Composition, wt percent			Temp., °C	Phases present
MgO	TiO_2	Fe_2O_3*		
11.1	49.4	39.5	1515	P + S
12.0	28.0	60.0	1505	α' + S
12.0	38.0	50.0	1520	α' + P + S
12.0	58.0	30.0	1580	P + L
			1552	P + L
			1545	P + minor S
			1540	P + S
12.0	68.0	20.0	1590	P + R
12.1	48.4	39.5	1515	P + S
12.1	61.2	26.7	1589	minor P + L
13.0	37.0	50.0	1520	P + α' + S
13.4	26.6	60.0	1585	S + L
			1566	S + L
			1520	α' + S
14.0	6.0	80.0	1515	S
14.1	27.9	58.0	1516	S + α'
14.1	46.4	39.5	1564	L
			1561	tr P + tr S + L
			1545	P + S + tr L
14.1	65.9	20.0	1631	L
			1518	P + tr S
14.8	29.2	56.0	1597	S + L
			1519	α' + P + S
			1499	α' + P + S
15.0	65.0	20.0	1582	P + L
			1576	P + tr L
			1554	P + S
15.1	45.4	39.5	1569	tr S + L
15.4	30.6	54.0	1565	S + L
			1513	S + P
16.0	54.0	30.0	1579	P + L
16.1	31.9	52.0	1520	S + P
16.1	44.4	39.5	1575	S + L
16.1	70.6	13.3	1598	P
16.8	33.2	50.0	1586	S + L
			1513	P + S
17.0	23.0	60.0	1695	S + L
			1612	S + L
			1526	S + P + α'
			1502	S + P + α'
17.0	53.0	30.0	1586	L
			1578	P + S + L
17.0	63.0	20.0	1620	L
			1591	P + L
18.0	52.0	30.0	1580	L
			1578	tr S + L
18.1	75.2	6.7	1610	P
19.0	21.0	60.0	1740	L
			1728	S + L
			1636	S + L
			1497	S + P
19.0	61.0	20.0	1569	P + S
19.0	71.2	9.8	1594	P + L
			1586	P + L
			1582	P + S
19.0	72.2	8.8	1580	P + S
19.0	74.0	7.0	1586	P + α
20.0	10.0	70.0	1527	S
20.0	72.2	7.8	1606	P + L
			1582	P + α + S
20.1	39.9	40.0	1568	S + L
			1565	P + S + tr L
			1553	P + S + tr L
			1548	P + S
21.0	19.0	60.0	1755	W + L
			1739	W + L
			1729	S + minor L + W
			1524	S + tr L
			1502	S + P
21.0	59.0	20.0	1594	P + L
			1572	P + S
22.0	58.0	20.0	1597	L
			1593	L + tr S
23.0	17.0	60.0	1731	S + tr W + tr L
			1723	S + tr L
			1546	S
23.0	57.0	20.0	1621	L
			1599	S + L
			1570	P + S
23.1	61.4	15.5	1616	L
			1594	S + P + L
			1588	S + P + L
			1580	S + P + tr L
23.1	67.1	9.8	1602	P + L
			1601	P + L
			1580	P + S
24.0	65.0	11.0	1566	P + S
25.0	15.0	60.0	1752	W + tr L
			1735	S + minor W
			1670	S
			1515	S
25.0	55.0	20.0	1609	S + L
			1515	P + S

TABLE 2 (continued)

Composition, wt percent			Temp., °C	Phases present
MgO	TiO_2	Fe_2O_3*		
25.1	65.1	9.8	1614	L
			1603	L + tr P
			1602	P + L
			1597	P + S + L
			1593	P + S +
			1579	P + α + S
			1552	P + S + α
26.0	34.0	40.0	1750	S + W + L
			1742	S + L
26.0	65.0	9.0	1620	L
			1597	α + P + L
			1593	α + P + tr L
			1585	α + P + S
			1583	α + P + S
			1568	α + P + S
26.0	69.0	5.0	1618	P + L
26.1	64.1	9.8	1608	tr S + L
26.2	9.9	63.9	1723	S + W
26.6	63.0	10.4	1613	S + L
26.8	53.2	20.0	1600	minor S + L
			1567	P + S
27.0	68.0	5.0	1621	L
			1612	α + P + L
			1610	α + P + minor L
28.0	32.0	40.0	1756	W + L
			1751	W + L
			1750	S + W + L
28.0	67.1	4.9	1622	L
			1618	α + L
			1610	α + L
28.1	62.1	9.8	1615	S + L
			1596	S + P + α
28.8	57.2	14.0	1588	P + S
29.0	11.0	60.0	1524	S + W
29.0	66.0	5.0	1621	L
			1620	L + tr S
			1618	S + L
			1618	α + L
			1593	α + P
29.1	57.9	13.0	1595	S + L
			1577	S + P
29.5	58.5	12.0	1606	S + L
			1595	S + P + L
			1589	S + P + α
			1577	S + P + α
30.0	62.0	8.0	1606	S + L
			1601	S + L + α
			1588	
30.0	64.8	5.2	1620	S + L
30.0	64.8	5.2	1605	α + L
30.2	59.8	10.0	1610	S + L
			1590	α + P + S
			1583	α + P + S
30.3	30.2	39.5	1589	S + L
			1569	S + L
			1560	S + L
			1551	S + tr L
			1544	S + P
			1530	S + P
30.6	60.6	8.8	1577	α + minor S
30.9	61.1	8.0	1591	α + S
31.0	9.0	60.0	1745	W + L
			1524	S + W
31.0	64.0	5.0	1623	S + L
			1615	α + minor S + L
31.5	62.5	6.0	1618	S + L
			1588	α + S
32.2	19.9	47.9	1734	W + S + minor L
			1730	W + S + minor L
			1719	S + W
33.3	50.2	16.5	1554	S + P
34.4	44.6	21.0	1763	tr W + L
			1761	W + L
			1757	S + L
			1752	S + L
			1631	S + L
35.0	5.0	60.0	1740	W
35.0	35.0	30.0	1589	S + minor L
			1580	S + L
			1546	S + L
35.0	50.0	15.0	1566	S + P
			1555	S + P
35.0	60.0	5.0	1629	S + L
36.1	54.1	9.8	1612	S + α + L
			1521	α + S
37.0	43.0	20.0	1763	W + L
			1759	S + L
			1729	S + L
			1558	S + P
37.0	49.5	13.5	1551	S + α
38.1	43.1	18.8	1583	S + L
38.2	29.9	31.9	1739	S + W
			1739	S + W
38.3	22.2	39.5	1751	W + L
			1741	W + S + L
			1721	W + S

TABLE 2 (continued)

Composition, wt percent			Temp., °C	Phases present	Composition, wt percent			Temp., °C	Phases present
MgO	TiO_2	Fe_2O_3*			MgO	TiO_2	Fe_2O_3*		
39.0	41.0	20.0	1583	S + L	44.2	39.8	16.0	1742	S + W + minor L
			1560	S + L				1741	S + minor W
			1554	S + α					
			1537	S + α	52.5	21.0	26.5	1738	W
40.0	41.0	19.0	1547	S + α	55.0	17.0	28.0	1738	W
40.0	43.0	17.0	1547	S + α	58.0	13.0	29.0	1739	W
41.0	41.0	18.0	1550	S + L	59.0	11.0	30.0	1738	W
			1541	S + tr P				1668	W
44.1	46.1	9.8	1591	S + L	60.5	9.0	30.5	1735	W
			1581	S + tr L					
			1578	S + tr L	64.8	2.9	32.3	1738	W
			1567	S + α				1619	W
44.2	39.8	16.0	1756	W + S + L	76.0	7.0	17.0	1750	W

*Total iron oxide calculated as Fe_2O_3.

Abbreviations: R, rutile; P, pseudobrookite solid solution; α, geikielite solid solution; α', hematite solid solution; S, spinel solid solution; W, magnesiowüstite; L, liquid; tr, trace.

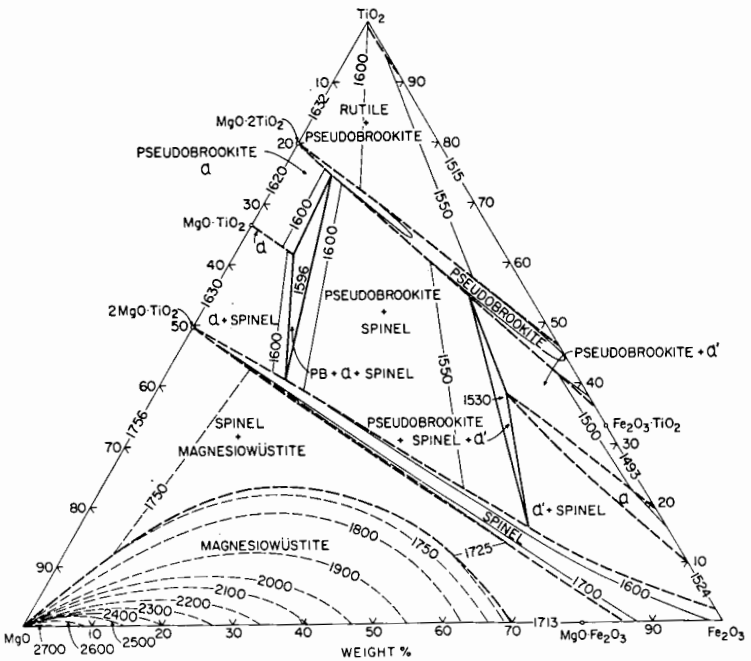

Fig. 7. Approximate 1300°C isothermal section of the system MgO–iron oxide–TiO_2 in air. Abbreviations used have the following meanings: α = geikielite solid solution, α' = hematite solid solution, PB = pseudobrookite solid solution, S = spinel.

TABLE 3

Results of equilibration runs for determination of subsolidus isothermal sections in the system MgO-iron oxide-TiO_2 in air

Temperature, °C	Composition, weight percent			Run duration, hours	Phases present
	MgO	TiO_2	Fe_2O_3*		
1700	31.0	9.0	60.0	8	W + tr S
	32.0	4.0	64.0	4	W
	32.0	4.0	64.0	10	W
	33.0	0.0	67.0	10	W
	33.0	7.0	60.0	5	W
	35.0	5.0	60.0	4	W
	40.0	17.0	43.0	5	W + tr S
	41.0	15.0	44.0	7	W
	45.0	20.0	35.0	5	W
	51.0	23.0	26.0	10	W + S
	53.0	21.0	26.0	10	W
	60.0	18.0	22.0	5	W
	68.0	15.0	17.0	6	W
	80.0	12.0	8.0	4	W + S
	90.0	4.0	6.0	10	W
	90.0	6.0	4.0	6	W + S
	94.0	2.0	4.0	5	W
	94.0	4.0	2.0	4	W + S
1650	32.5	4.0	63.5	8	W + S
	39.0	10.0	51.0	12	W
	40.0	5.0	55.0	6	W
	41.0	15.0	44.0	10	W + S
	44.0	15.0	41.0	8	W
	47.0	18.0	35.0	4	W + S
	49.0	16.0	35.0	6	W
	55.0	17.0	28.0	5	W + S
	59.0	11.0	30.0	10	W
	60.0	18.0	22.0	7	W + S
	62.0	16.0	22.0	6	W + S
	68.0	15.0	17.0	8	W + S
	70.0	12.0	18.0	8	W + tr S
	80.0	8.0	12.0	8	W
	80.0	12.0	8.0	6	W + S
	90.0	4.0	6.0	8	W + tr S
	90.0	6.0	4.0	5	W + S
	94.0	2.0	4.0	5	W + tr S
	94.0	4.0	2.0	6	W + S
1600	45.0	5.0	50.0	8	W
	59.0	11.0	30.0	10	W + S
	72.0	8.0	20.0	8	W
1500	55.0	3.0	42.0	11	W + S
	57.0	1.0	42.0	8	W
	61.0	4.0	35.0	10	W + S
	64.5	3.0	32.5	15	W
	67.0	3.0	30.0	12	W
	75.0	3.0	22.0	10	W + tr S
	76.0	6.0	18.0	12	W + S
	79.0	4.0	17.0	10	W + tr S
	85.0	3.0	12.0	14	W + tr S
	89.0	2.0	9.0	10	W
	90.0	4.0	6.0	16	W + S
	94.0	1.0	5.0	15	W
	94.0	2.0	4.0	18	W + S
1400	68.0	2.0	30.0	20	W + S
	69.0	1.0	30.0	22	W + S
	70.0	0.0	30.0	20	W
	74.0	2.0	24.0	18	W
	75.0	3.0	22.0	22	W + S
	79.0	4.0	17.0	24	W + S
	81.0	1.0	18.0	20	W
	85.0	3.0	12.0	36	W + S
	89.0	2.0	9.0	18	W

TABLE 3 (continued)

Temperature, °C	Composition, weight percent			Run duration, hours	Phases present
	MgO	TiO_2	Fe_2O_3*		
1400	90.0	4.0	6.0	18	W + S
	94.0	2.0	4.0	20	W + S
1300	3.0	7.0	90.0	168	α' + S
	4.0	43.0	53.0	168	P
	6.0	24.0	70.0	168	P + α'
	7.0	13.0	80.0	168	S + α'
	7.0	27.0	66.0	168	P + α'
	12.0	61.0	27.0	168	P
	14.0	16.0	70.0	168	α' + S
	14.0	28.0	58.0	168	α' + P + S
	15.0	29.0	56.0	168	α' + P + S
	15.0	31.0	54.0	168	P + S
	16.0	32.0	52.0	168	P + S
	17.0	58.0	25.0	168	P + S
	20.0	20.0	60.0	168	α' + P + S
	20.0	40.0	40.0	168	P + S
	20.0	50.0	30.0	168	P + S
	20.0	58.0	22.0	168	α + P + S
	26.0	10.0	64.0	168	S
	26.0	52.0	22.0	168	α + P + S
	27.0	53.0	20.0	168	α + P + S
	28.0	62.0	10.0	168	α + P
	29.0	11.0	60.0	168	S + W
	31.0	62.0	7.0	168	
	31.0	64.0	5.0	168	α + tr P
	32.0	48.0	20.0	168	α + S
	33.0	45.0	22.0	168	α + S
	35.0	60.0	5.0	168	α + S
	36.0	54.0	10.0	168	α + S
	37.0	35.0	28.0	168	P + S
	38.0	30.0	32.0	168	S
	38.0	40.0	22.0	168	α + S
1000	9.0	23.0	68.0	504	α' + tr P
	9.0	35.0	56.0	504	α' + P
	10.0	10.0	80.0	504	α' + S
	10.0	20.0	70.0	504	α' + S
	10.0	30.0	60.0	504	α' + P
	12.0	50.0	38.0	504	S + P
	14.0	28.0	58.0	504	α' + P + S
	15.0	30.0	55.0	504	α' + P + S
	15.0	50.0	35.0	504	α + P + S
	16.0	26.0	58.0	504	α' + P + S
	20.0	20.0	60.0	504	S + P
	20.0	30.0	50.0	504	S + P
	20.0	40.0	40.0	504	α + P + S
	20.0	60.0	20.0	504	α + P
	20.0	58.0	22.0	504	α + P
	22.0	38.0	40.0	504	α + P + S
	23.0	36.0	41.0	504	α + P + S
	24.0	42.0	34.0	504	α + P + S
	24.0	52.0	24.0	504	α + P
	25.0	30.0	45.0	504	S + P
	26.0	52.0	22.0	504	α
	30.0	30.0	40.0	504	α + S
	31.0	62.0	7.0	504	α
	32.0	40.0	28.0	504	α + S
	33.0	45.0	22.0	504	α + S
	37.0	35.0	28.0	504	α + S

*Total iron oxide calculated as Fe_2O_3.

Abbreviations: R, rutile; P, pseudobrookite solid solution; α, geikielite solid solution; α', hematite solid solution; W, magnesiowüstite; S, spinel solid solution; L, liquid; tr, trace.

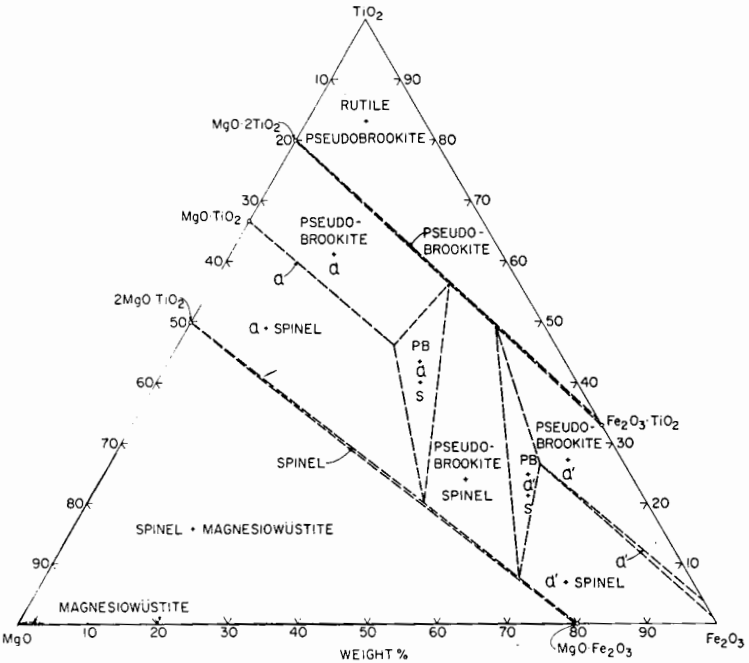

Fig. 8. Approximate 1000°C isothermal section of the system MgO–iron oxide–TiO_2 in air. Abbreviations used have the following meanings: α = geikielite solid solution, α' = hematite solid solution, PB = pseudobrookite solid solution, S = spinel.

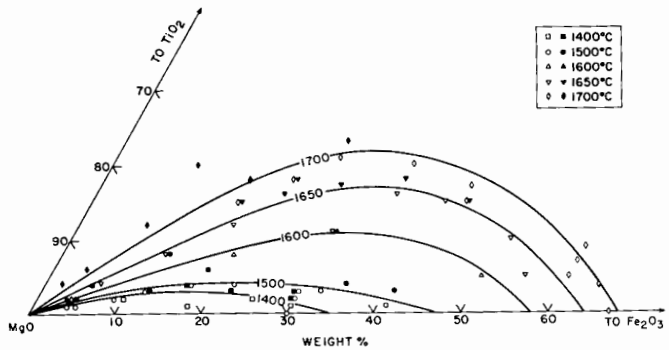

Fig. 9. Diagram showing the solubility of TiO_2 in magnesiowüstite as a function of temperature in the system MgO–iron oxide–TiO_2 in air. Open symbols represent mixtures in the one-phase area of magnesiowüstite at the various temperatures, and solid symbols represent mixtures in the two-phase area magnesiowüstite plus spinel.

ACKNOWLEDGMENT

The present work was sponsored by the American Iron and Steel Institute.

REFERENCES

Corruccini, R. J., 1949, Differences between international temperature scales of 1948 and 1927: Natl. Bur. Standards Research Jour., v. 43, p. 133-136, RP 2014.

Coughanour, L. W., and DeProsse, V. A., 1953, Phase equilibria in the system MgO–TiO_2: Natl. Bur. Standards Research Jour., v. 51, p. 85-88.

Elliott, J. F., and Gleiser, M., 1960, Thermochemistry for steelmaking, v. 1: Reading, Mass., Addison-Wesley Publishing Company, Inc.

MacChesney, J. B., and Muan, A., 1959, Studies in the system iron oxide-titanium oxide: Am. Mineralogist, v. 44, p. 926-945.

Massazza, F., and Sirchia, E., 1958, The system MgO–SiO_2–TiO_2. 1. Revision of the binary systems: Chim. Ind. (Milan), v. 40, p. 376-380.

Muan, A., and Osborn, E. F., 1956, Phase equilibria at liquidus temperatures in the system MgO–FeO–Fe_2O_3–SiO_2: Am. Ceramic Soc. Jour., v. 39, p. 121-140.

———— 1965, Phase equilibria among oxides in steelmaking: Reading, Mass., Addison-Wesley Publishing Company, Inc.

Phillips, B., Sōmiya, S., and Muan, A., 1961, Melting relations of magnesium oxide-iron-oxide mixtures in air: Am. Ceramic Soc. Jour., v. 44, p. 167-169.

Shepherd, E. S., Rankin, G. A., and Wright, F. E., 1909, Binary systems of alumina with silica, lime, and magnesia: Am. Jour. Sci., 4th ser., v. 28, p. 293-333.

Sosman, R. B., 1952, Temperature scales and silicate research: Am. Jour. Sci., Bowen v., pt. 2, p. 517-528.

Willshee, J., and White, J., 1967, An investigation of equilibrium relationships in the system MgO–FeO–Fe_2O_3 to 1750° in air: British Ceramic Soc. Trans., v. 66, p. 541-555.